

Determination of Absolute Configuration Using Vibrational Circular Dichroism Spectroscopy: The Chiral Sulfoxide 1-(2-methylnaphthyl) Methyl Sulfoxide

P. J. Stephens,* A. Aamouche, and F. J. Devlin

Department of Chemistry, University of Southern California, Los Angeles, California 90089-0482

S. Superchi, M. I. Donnoli, and C. Rosini

Dipartimento di Chimica, Università della Basilicata, Via N. Sauro 85, 85100 Potenza, Italy

stephens@chem1.usc.edu

Received September 22, 2000

We report the determination of the absolute configuration (AC) of the chiral sulfoxide, 1-(2-methylnaphthyl) methyl sulfoxide, **1**, using vibrational circular dichroism (VCD) spectroscopy. The VCD of **1** has been measured in the mid-IR spectral region in CCl₄ solution. Analysis employs the ab initio DFT/GIAO methodology. DFT calculations predict two stable conformations of **1**, *E* and *Z*, *Z* being lower in energy than *E* by <1 kcal/mol. In both conformations the S–O bond is rotated from coplanarity with the naphthyl moiety by 30–40°. The predicted unpolarized absorption (“IR”) spectrum of the equilibrium mixture of the two conformations permits assignment of the experimental IR spectrum in the mid-IR spectral region. The presence of both *E* and *Z* conformations is clearly evident. The VCD spectrum predicted for *S*-**1** is in excellent agreement with the experimental spectrum of (–)-**1**, unambiguously defining the AC of **1** as *R*(+)/*S*(–).

Introduction

Chiral molecules exhibit vibrational circular dichroism (VCD).¹ VCD was first observed in the 1970s.² Subsequently, instrumentation for the measurement of VCD spectra has developed greatly in frequency range and sensitivity.³ Currently, VCD spectra of liquids and solutions can be measured over the majority of the fundamental infrared (IR) spectral range ($\bar{\nu} \geq 650 \text{ cm}^{-1}$) using both dispersive and Fourier transform (FT) instrumentation.

The VCD spectrum of a chiral molecule reflects its three-dimensional structure. Most importantly, VCD is a function of the absolute configuration (AC). The enantiomers of a chiral molecule exhibit mirror-image VCD spectra, i.e., at any frequency the VCD intensities of the two enantiomers are equal in magnitude and opposite in sign. As a result, in principle, the VCD spectrum of a chiral molecule of unknown AC allows the determination of its AC.

To date, organic chemists have made negligible use of VCD spectroscopy in determining the ACs of chiral molecules. This can be attributed to some extent to the limited availability of VCD instrumentation. However, more importantly, there has not been available a routine,

reliable methodology permitting the extraction of structural information from VCD spectra. Consequently, even if VCD spectra were measured, ACs could not be easily and reliably deduced.

Very recently, two developments have radically changed the practical applicability of VCD spectroscopy to the determination of AC. First, commercial FT instrumentation for the measurement of VCD spectra has become available, greatly enhancing the accessibility of the technique. Second, a theoretical methodology has been developed and implemented,⁴ permitting for the first time the routine, reliable prediction of VCD spectra.^{1,5} This methodology uses ab initio density functional theory (DFT),⁶ whose power is by now familiar to many organic chemists, and gauge-invariant atomic orbitals (GIAOs),⁷ widely used in ab initio calculations of NMR shielding constants. The implementation of this DFT/GIAO methodology within the widely used ab initio quantum chemistry package GAUSSIAN⁸ optimizes its accessibility. Thus, at this time the application of VCD spectroscopy to the determination of the AC of a chiral molecule has become straightforward.^{1,9}

(1) (a) Stephens, P. J.; Devlin, F. J. *Chirality*, **2000**, *12*, 172. (b) Stephens, P. J.; Devlin, F. J.; Aamouche, A. *Physical Chemistry of Chirality*; ACS Symposium Series; American Chemical Society: Washington, DC, 2000, in press.

(2) (a) Holzwarth, G.; Hsu E. C.; Mosher, H. S.; Faulkner, T. R.; Moscovitz, A. *J. Am. Chem. Soc.* **1974**, *96*, 251. (b) Nafie, L. A.; Cheng, J. C.; Stephens, P. J. *J. Am. Chem. Soc.* **1975**, *97*, 3842. (c) Nafie, L. A.; Keiderling, T. A.; Stephens, P. J. *J. Am. Chem. Soc.* **1976**, *98*, 2715.

(3) (a) Nafie, L. A. In *Advances in Fourier Transform Spectroscopy*; Mackenzie M. W., Ed., Wiley: New York, 1988; p 67. (b) Keiderling, T. A. In *Practical Fourier Transform Infrared Spectroscopy*; Academic Press: New York, 1990; p 203.

(4) Cheeseman, J. R.; Frisch, M. J.; Devlin, F. J.; Stephens P. J. *Chem. Phys. Lett.* **1996**, *252*, 211.

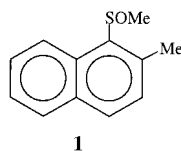
(5) (a) Stephens, P. J.; Ashvar, C. S.; Devlin, F. J.; Cheeseman, J. R.; Frisch, M. J. *Mol. Phys.* **1996**, *89*, 579. (b) Devlin, F. J.; Stephens, P. J.; Cheeseman, J. R.; Frisch, M. J. *J. Phys. Chem.* **1997**, *101*, 6322. (c) Devlin, F. J.; Stephens, P. J.; Cheeseman, J. R.; Frisch, M. J. *J. Phys. Chem.* **1997**, *101*, 9912. (d) Ashvar, C. S.; Devlin, F. J.; Stephens, P. J.; Bak, K. L.; Eggimann, T.; Wieser, H. *J. Phys. Chem.* **1998**, *102*, 6842. (e) Ashvar, C. S.; Devlin, F. J.; Stephens, P. J. *J. Am. Chem. Soc.* **1999**, *121*, 2836.

(6) Laird, B. B.; Ross, R. B.; Ziegler, T., Eds. *Chemical Applications of Density Functional Theory*; ACS Symposium Series 629; American Chemical Society: Washington, DC, 1996.

(7) (a) London, F. *J. Phys. Radium* **1937**, *8*, 397. (b) Ditchfield, R. *Mol. Phys.* **1974**, *27*, 789.

(8) Frisch, M. J. et al. *Gaussian 98*, Gaussian Inc., Pittsburgh, PA.

In this paper, we illustrate the utilization of VCD spectroscopy to determine AC using the specific case of a chiral sulfoxide, 1-(2-methylnaphthyl) sulfoxide, **1**:

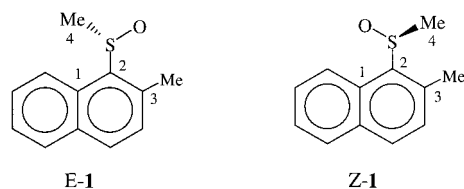


Chiral sulfoxides are of considerable importance as bioactive compounds,¹⁰ synthetic intermediates,¹¹ and ligands¹² for asymmetric synthesis. Much effort has been devoted to the development of methods for synthesizing chiral sulfoxides of high enantiomeric purity.¹³ To date, chiroptical methods have found limited application in determining the ACs of chiral sulfoxides.¹⁴ We have therefore recently initiated studies of chiral sulfoxides using VCD spectroscopy.¹⁵ One group of sulfoxides under study are aryl alkyl sulfoxides in which the aryl group is a naphthyl or substituted naphthyl group. The chiral sulfoxide **1**, one of the molecules in this group under study, has been synthesized previously by Casarini et al. and its enantiomers resolved using chiral chromatography.¹⁶ However, no chiroptical data were reported, including optical rotation data, and the AC of **1** remains undefined. We have therefore determined the AC of **1** using VCD spectroscopy, and here report our results.

The VCD protocol can be summarized as follows. First, the VCD spectrum of the molecule of interest is measured in solution in an appropriate solvent, together with the vibrational unpolarized absorption spectrum ("the IR

spectrum"). Second, the stable conformations of the molecule are predicted using DFT. Third, the IR and VCD spectra of all conformations predicted to be significantly populated at room temperature are calculated using DFT and conformationally averaged spectra derived thence. Fourth, the predicted IR spectrum is used to assign the experimental IR spectrum. Fifth, for unambiguously assigned bands of the IR spectrum, the predicted VCD is compared to the experimental VCD in order to determine the AC. In principle, it is only necessary to use one vibrational transition to assign the AC of a molecule from its VCD spectrum. However, the reliability of the conclusion increases as the number of transitions utilized increases.

It is important to note that in addition to the AC of the molecule of interest, our protocol simultaneously defines the structures and relative energies of its conformations. Thus, conformational analysis is an automatic byproduct of the determination of AC.^{1,17} In the case of **1**, NMR studies by Casarini et al.¹⁶ of **1** in CD₂-Cl₂ solution provided evidence of two conformations, *E*-**1** and *Z*-**1** in equilibrium. Temperature-dependent NMR



studies found a 88:12 ratio of the two conformations at -90°C , corresponding to a free energy difference of 0.73 kcal/mol, and a barrier to conformational interconversion of 10.6 kcal/mol. Chemical shift differences for the two conformations led to the conclusion that the *Z* conformation is the more stable. This conclusion was supported by NOE and LIS studies of 1-(2-methylnaphthyl) *tert*-butyl sulfoxide. The studies reported here both confirm the qualitative conclusions of Casarini et al. and yield a quantitative description of the structures of the *E* and *Z* conformations of **1**.

Results and Discussion

(+)-**1** and (–)-**1** were synthesized by asymmetric oxidation of 1-(2-methylnaphthyl) methyl sulfide using *t*-BuOOH in the presence of Ti(*i*-PrO)₄, H₂O, and enantiopure 1,2-diphenylethane-1,2-diol (DPED).^{13f,18} (–)-**1** was obtained using (*R,R*)-DPED in 45% chemical yield and 60% ee, while oxidation with (*S,S*)-DPED afforded (+)-**1** in 50% yield and 50% ee.

The determination of the AC of **1** begins with the measurement of its VCD spectrum. In this work, we have used a ~ 0.1 M solution of **1** in CCl₄. CCl₄ is a good IR solvent, i.e., strong CCl₄ absorption, preventing VCD measurement, is limited to a relatively small fraction of the IR spectral region. In addition, solute–solvent interactions are minimized. In particular, specific solute–solvent interactions, such as hydrogen-bonding, are absent. This is of importance since solute–solvent inter-

(9) (a) Aamouche, A.; Devlin, F. J.; Stephens, P. J. *J. Chem. Soc., Chem. Commun.* **1999**, 361. (b) Aamouche, A.; Devlin, F. J.; Stephens, P. J. *J. Am. Chem. Soc.* **2000**, *122*, 2346.

(10) For recent examples, see: (a) Cotton, H.; Elebring, T.; Larsson, M.; Li, L.; Sorensen, H.; von Unge, S. *Tetrahedron: Asymmetry* **2000**, *11*, 3819. (b) Padmanabhan, S.; Lavin, R. C.; Durant, G. J. *Tetrahedron: Asymmetry* **2000**, *11*, 3455.

(11) (a) Carreño, M. C. *Chem. Rev.* **1995**, *95*, 1717. (b) Solladié, G. *Synthesis* **1981**, 185. (c) Posner, G. H. In *The Chemistry of Sulfones and Sulfoxides*; Patai, S., Rappoport, Z., Stirling, C. J. M., Eds.; Wiley: Chichester, England, 1988; Chapter 16, pp 823–849. (d) Colobert, F.; Tito, A.; Khair, N.; Denni, D.; Medina, M. A.; Martin-Lomas, M.; Ruano, J. L. G.; Solladié, G. *J. Org. Chem.* **1998**, *63*, 8918.

(12) (a) Hiroi, K.; Suzuki, Y. *Tetrahedron Lett.* **1998**, *39*, 6499. (b) Tokunoh, R.; Sodeoka, M.; Aoe, K.; Shibasaki, M. *Tetrahedron Lett.* **1995**, *36*, 8035. (c) Khair, N.; Fernandez, I.; Alcudia, F. *Tetrahedron Lett.* **1993**, *34*, 123.

(13) (a) Andersen, K. K. In *The Chemistry of Sulfones and Sulfoxides*; Patai, S., Rappoport, Z., Stirling, C. J. M., Eds.; Wiley: Chichester, England, 1988; Chapter 3, pp 53–94. (b) Kagan, H. B. In *Catalytic Asymmetric Synthesis*; Ojima, I., Ed.; VCH: New York, 1993; pp 203–226. For recent examples of chemical asymmetric sulfoxidations, see: (c) Brunel, J.-M.; Diter, P.; Duetsch, M.; Kagan, H. B. *J. Org. Chem.* **1995**, *60*, 8086. (d) Komatsu, N.; Hashizume, M.; Sugita, T.; Uemura, S. *J. Org. Chem.* **1993**, *58*, 4529. (e) Di Furia, F.; Licini, G.; Modena, G.; Motterle, R.; Nugent, W. A. *J. Org. Chem.* **1996**, *61*, 5175. (f) Superchi, S.; Rosini, C. *Tetrahedron: Asymmetry* **1997**, *8*, 349. (g) Yamanoi, Y.; Imamoto, T. *J. Org. Chem.* **1997**, *62*, 8560. (h) Bolm, C.; Dabard, O. A. G. *Synlett* **1999**, *3*, 360.

(14) For studies of the optical rotatory dispersion and circular dichroism of chiral sulfoxides in the visible-UV spectral region, see, for example: (a) Mislow, K.; Green, M. M.; Laur, P.; Melillo, J. T.; Simmons, T.; Ternay, A. L. *J. Am. Chem. Soc.* **1965**, *87*, 1958. (b) Bendazzoli, G. L.; Palmieri, P.; Gottarelli, G.; Moretti, I.; Torre, G. *J. Am. Chem. Soc.* **1976**, *98*, 2659. (c) Moretti, I.; Torre, G.; Gottarelli, G. *Tetrahedron Lett.* **1976**, 711. (d) Bendazzoli, G. L.; Palmieri, P.; Gottarelli, G.; Moretti, I.; Torre, G. *Gazz. Chim. Ital.* **1979**, *109*, 19. (e) Rosini, C.; Donnoli, M. I.; Superchi, S. *Chem.-Eur. J.* **2001**, *7*, 72.

(15) (a) Aamouche, A.; Devlin, F. J.; Stephens, P. J.; Drabowicz, J.; Bujnicki, B.; Mikolajczyk, M. *Chem.-Eur. J.* **2000**, *6*, 4479. (b) Aamouche, A.; Devlin, F. J.; Stephens, P. J.; Superchi, S.; Donnoli, M. I.; Rosini, C., to be submitted.

(16) Casarini, D.; Foresti, E.; Gasparrini, F.; Lunazzi, L.; Macciantelli, D.; Misiti, D.; Villani, C. *J. Org. Chem.* **1993**, *58*, 5674.

(17) For applications of VCD spectroscopy to conformational analysis using the DFT/GIAO methodology, see: (a) Devlin, F. J.; Stephens, P. J. *J. Am. Chem. Soc.* **1999**, *121*, 7413. (b) Aamouche, A.; Devlin, F. J.; Stephens, P. J. *J. Am. Chem. Soc.* **2000**, *122*, 7358.

(18) (a) Superchi, S.; Donnoli, M. I.; Rosini, C. *Tetrahedron Lett.* **1998**, *39*, 8541. (b) Donnoli, M. I.; Superchi, S.; Rosini, C. *J. Org. Chem.* **1998**, *63*, 9392. (c) Donnoli, M. I.; Superchi, S.; Rosini, C. *Enantiomer* **2000**, *5*, 181.

actions are not included in the theoretical methodology. Last, **1** exhibits good solubility in CCl_4 . Optimum VCD signal-to-noise ratios are obtained with IR absorbances in the range 0.1–1.0 and with the shortest possible path lengths (to minimize solvent absorption). The higher the solution concentration, the lower the path length that can be used. However, it is important that spectra reflect monomeric solute molecules and not dimeric or more highly aggregated solute species, since the theoretical calculations with which they are to be compared are for single molecules. Thus, VCD measurements must be made within the concentration range over which Beer's law is obeyed. Sulfoxides are known to aggregate in nonpolar solvents.^{15a} We have shown that the IR spectrum of **1** in CCl_4 satisfies Beer's Law up to concentrations ~ 0.1 M (see Methods, below) and have therefore used a ~ 0.1 M solution for VCD measurement.

We have measured the VCD of **1** in the mid-IR spectral region. With few exceptions, the C–H stretching modes of organic molecules give rise to complex, poorly resolved spectra which are difficult to analyze. Mid-IR spectra are simpler and more easily analyzed. Mid-IR VCD has been measured using a commercial FT VCD spectrometer, whose lower frequency limit is ~ 700 cm^{-1} . Using CCl_4 solutions, the lower frequency limit is > 800 cm^{-1} , due to strong CCl_4 absorption near 800 cm^{-1} . IR spectra have been measured simultaneously using a conventional FTIR spectrometer. The lower frequency limit (~ 300 cm^{-1}) of our IR spectra is imposed by the KBr windows of the cells utilized.

Experimental IR and VCD spectra of a 0.12 M CCl_4 solution of **1** in the mid-IR spectral range are shown in Figure 1. Over the frequency range studied, the VCD intensities of **1** vary widely. The VCD spectrum is dominated by two features at ~ 950 cm^{-1} and ~ 1070 cm^{-1} , respectively. The latter corresponds to the absorption band at ~ 1070 cm^{-1} , attributable to the S–O stretching vibration. Anisotropy ratios ($\Delta\epsilon/\epsilon = \Delta A/A$) are $\sim 2.7 \times 10^{-4}$ and $\sim 0.9 \times 10^{-4}$ for the ~ 950 cm^{-1} and ~ 1070 cm^{-1} bands, respectively. However, over much of the spectrum, VCD intensities are weaker, and for many vibrational transitions VCD was not detectable. In this regard, the VCD spectrum of **1** is quite different from that of the benchmark molecule α -pinene, which exhibits strong, easily measurable VCD across the entire mid-IR spectral region.^{5c}

The analysis of the VCD spectrum of **1** begins with the prediction of the stable conformations, accessible at room temperature. The stable conformations of **1** are predicted as follows. First, the potential energy surface (PES) is scanned, varying the dihedral angle OSC2C3, i.e., rotating the SOMe group with respect to the naphthyl moiety about the SC2 single bond. DFT, using the B3PW91 Becke hybrid functional¹⁹ and the 6-31G* basis set,²⁰ yields the results shown in Figure 2. As OSC2C3 is varied through 360° , two minima and two maxima are predicted. The two minima correspond to *E* and *Z* conformations, *Z* being lower in energy than *E*. The maxima lie 11–12 kcal/mol higher in energy than *Z*-**1**. Second, the structures of the *E* and *Z* conformations of **1** are obtained by unconstrained optimizations, using B3PW91 and the TZ2P basis set.²¹ The TZ2P basis set is much larger than

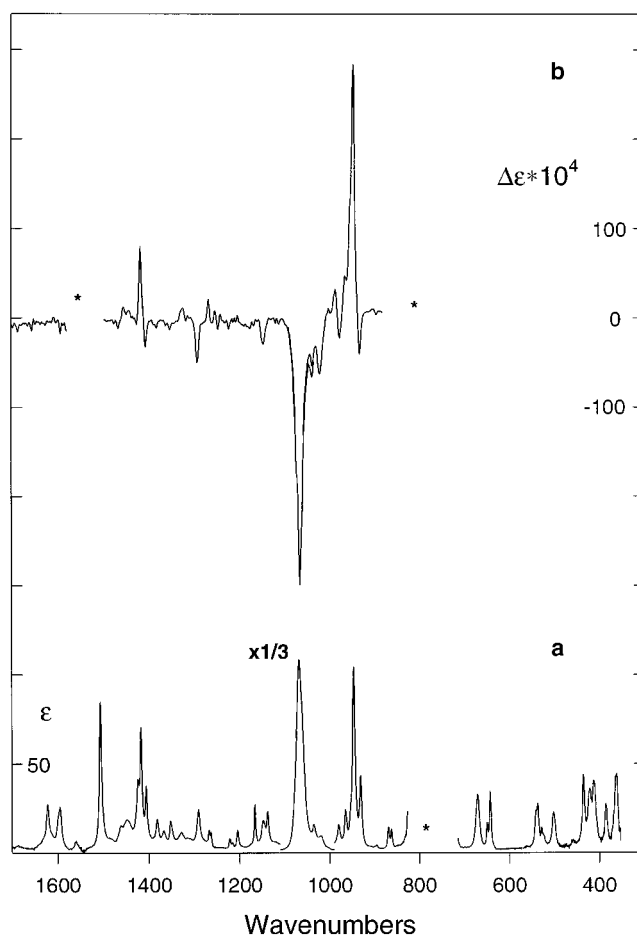


Figure 1. Mid-IR unpolarized absorption (IR) spectrum of (±)-**1**, **a**, and VCD spectrum of (–)-**1**, **b**, in CCl_4 solution (0.12 M). The VCD spectrum is the 100% ee “half-difference” spectrum (see text). The path lengths used were: **a**, 597 μm ; **b**, 597 μm (880–1057 cm^{-1} and 1076–1700 cm^{-1}) and 239 μm (1034–1090 cm^{-1}). Asterisks indicate regions of excessive CCl_4 absorption.

the 6-31G* basis set and, therefore, substantially more accurate. Key structural and energetic parameters for the B3PW91/TZ2P structures are reported in Tables 1 and 2. The B3PW91/TZ2P structures are displayed in Figure

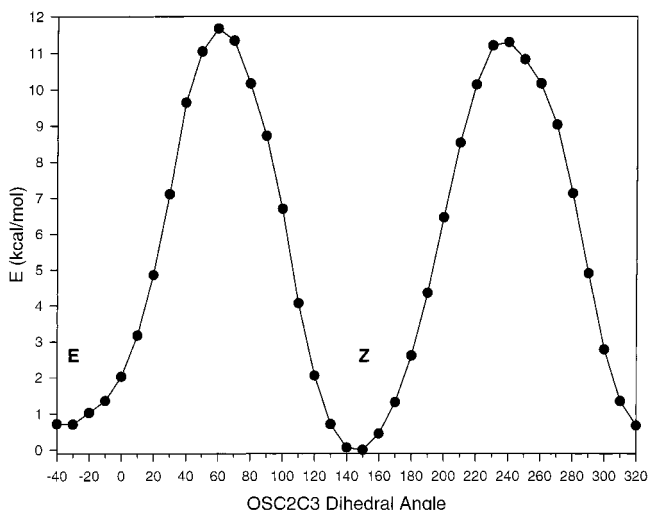


Figure 2. B3PW91/6-31G* Potential energy surface (PES) of **1** as a function of the OSC2C3 dihedral angle (atom numbering is indicated in the text).

(19) Becke, A. D. *J. Chem. Phys.* **1993**, *98*, 1372, 5648.

(20) Hehre, W. J.; Schleyer, P. R.; Radom, L.; Pople, J. A. *Ab Initio Molecular Orbital Theory*; Wiley: New York, 1986.

(21) Stephens, P. J.; Jalkanen, K. J.; Amos, R. D.; Lazzeretti, P.; Zanasi, R. *J. Phys. Chem.* **1990**, *94*, 1811.

Table 1. B3PW91/TZ2P Structural Parameters for **1**^a

coordinates ^b	<i>E</i> - 1	<i>Z</i> - 1
SO	1.501	1.502
SC2	1.827	1.821
SC4	1.822	1.825
C1C2	1.430	1.427
C2C3	1.381	1.383
OSC4	107.1	106.7
OSC2	110.8	111.3
C2SC4	97.1	96.8
C1C2S	115.7	122.3
C3C2S	122.6	115.8
C3C2C1	121.7	121.9
OSC2C1	144.7	-34.4
OSC2C3	-32.8	145.5
C4SC2C1	-103.9	76.6
C4SC2C3	78.6	-103.6

^a Bond lengths in angstroms; bond angles and dihedral angles in degrees. Dihedral angles are for the *S* absolute configuration.

^b Atom numbering is indicated in the text.

3. Bond angles at S are approximately tetrahedral; distortion from tetrahedral is greatest for C2SC4. In both conformations the S–O bond is rotated from coplanarity with the naphthyl moiety by 30–40°. The S–C4 bond is not far from perpendicular to the naphthyl plane. Bond lengths and bond angles of *E*- and *Z*-**1** are very similar; the largest differences are for the S–C2 bond length and for the C1C2S and C3C2S bond angles. The *E*–*Z* energy difference $\Delta E_{EZ} = E_E - E_Z$ is ~ 0.5 kcal/mol. Populations based on Boltzmann statistics are $\sim 70\%$ for *Z*-**1** and $\sim 30\%$ for *E*-**1**. Our results are in qualitative accord with the work of Casarini et al.¹⁶

Table 2. B3PW91/TZ2P Conformational Energy Differences and Populations for **1**–**4**^a

	1 ^d	3 ^e	4 ^f	3 – 4 ^g
ΔE^b	0.48	2.15	1.80	0.35
<i>P</i> ^c	69.2/30.8	98.0/2.0	95.4/4.6	

^a Energy differences, ΔE , in kcal/mol; populations, *P*, are percentages. ^b Energy difference of *E* and *Z* conformations. ^c Populations of lower energy/higher energy conformations. ^d *Z*-**1** is lower in energy than *E*-**1**. ^e *E*-**3** is lower in energy than *Z*-**3**. ^f *E*-**4** is lower in energy than *Z*-**4**. ^g Difference of conformational energy differences of **3** and **4**.

Given the structures of *E*- and *Z*-**1**, we have calculated their IR and VCD spectra using the B3PW91 functional and the TZ2P basis set. IR spectra of *E*- and *Z*-**1** in the mid-IR region are shown in Figure 4. Prediction of the

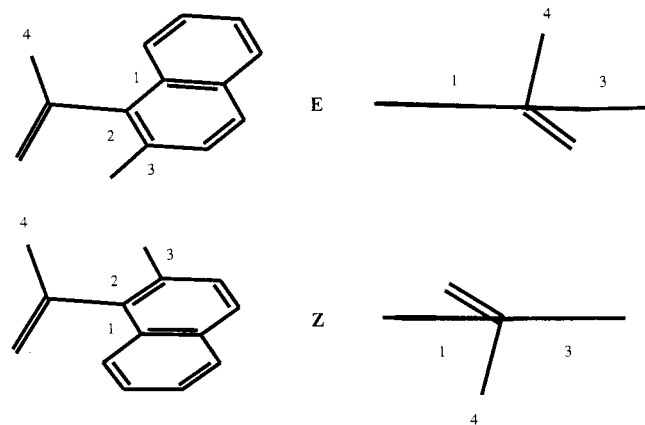


Figure 3. B3PW91/TZ2P structures of *E*-**1** and *Z*-**1**. H atoms are not shown. In the right-hand panel, **1** is viewed along the SC2 bond, the S atom being toward the viewer. The AC of **1** is *S*.

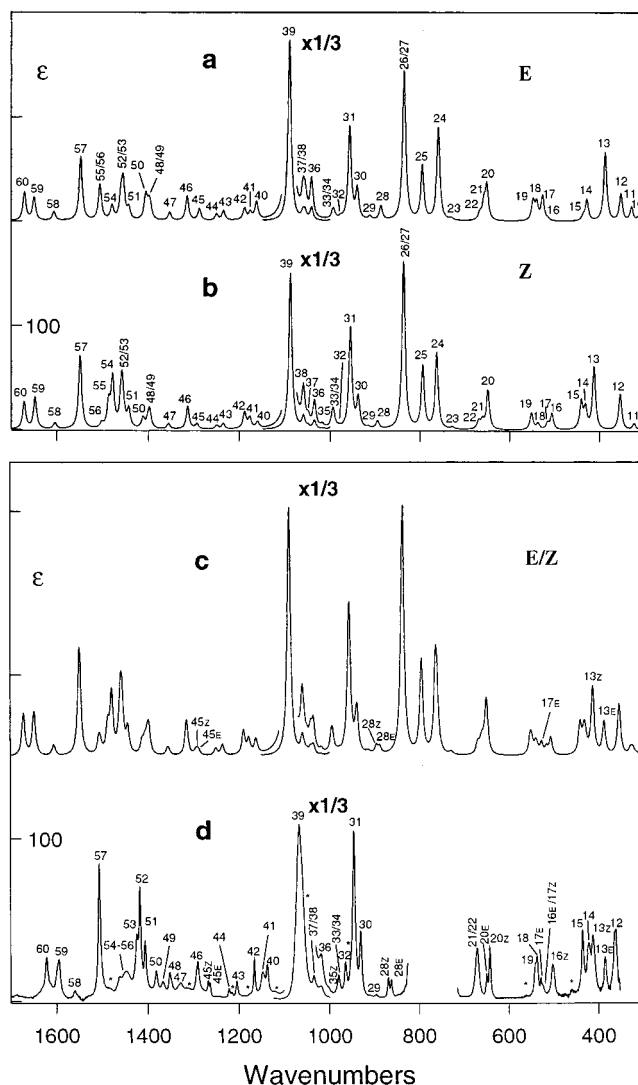


Figure 4. Mid-IR unpolarized absorption (IR) spectra of **1**. **a**: B3PW91/TZ2P spectrum of *E*-**1**; **b**: B3PW91/TZ2P spectrum of *Z*-**1**; **c**: B3PW91/TZ2P *E/Z* spectrum; **d**: experimental spectrum (from Figure 1). In **a** and **b** band shapes are Lorentzian; $\gamma = 4.0$ cm⁻¹. The spectrum in **c** is obtained from those in **a** and **b** using populations of *E*- and *Z*-**1** calculated from their B3PW91/TZ2P energies (Table 2). Fundamentals are numbered. In **d**, where *E* and *Z* bands are not resolved, the numbering refers to both *E* and *Z* conformations. In **d**, asterisks indicate bands not assignable to fundamentals of **1** and attributable to either overtone/combination bands of **1** or impurities.

spectra proceeds in two stages. First, vibrational frequencies and dipole strengths are calculated using GAUSSIAN 98.⁸ The results are given in Table 1 of Supporting Information. Second, spectra are synthesized using Lorentzian band shapes. (Liquid solution band shapes are generally Lorentzian to a good approximation.^{5b,c}) It is important to note that the calculations are carried out within the framework of the harmonic approximation (HA). Within the HA, only fundamental vibrational transitions are allowed. Accordingly, in an *N*-atom molecule predicted spectra contain $3N - 6$ fundamental transitions corresponding to the $3N - 6$ normal modes. In Figure 4, numbers indicate the fundamentals from which bands originate. Fundamentals are numbered in ascending frequency order. *E*- and *Z*-**1** are predicted to be in equilibrium at room temperature. The

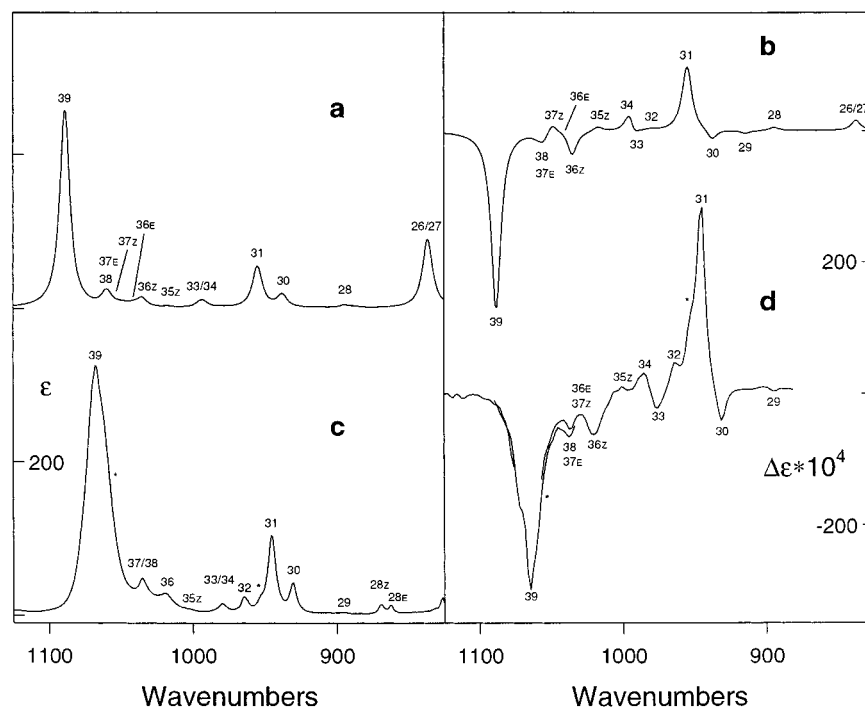


Figure 5. IR and VCD spectra originating in modes 28–39 of **1**. **a, b:** B3PW91/TZ2P *E/Z* spectra (from Figures 4 and 6); **c, d:** experimental spectra (from Figure 1).

IR spectrum of the conformational mixture is predicted assuming the populations of the *E* and *Z* conformations to be those obtained from the B3PW91/TZ2P energy difference, given in Table 2. The resulting *E/Z* spectrum is shown in Figures 4 and 5. The B3PW91/TZ2P mid-IR spectra of *E*- and *Z*-**1** are qualitatively very similar overall. The largest differences are for modes 13–15, 16–19, 36–38, and 54–56. These differences reflect differences in frequency and/or dipole strength. For modes 12–60, the largest differences in frequency are exhibited by modes 13 (25 cm⁻¹) and 55 (17 cm⁻¹). For the majority of fundamentals 12–60 the *E*–*Z* frequency differences are <5 cm⁻¹, comparable to or less than the vibrational bandwidth. As a result, the number of bands observed in the predicted *E/Z* spectrum is only slightly larger than observed in the individual *E* and *Z* spectra.

By comparison of the predicted *E/Z* IR spectrum to the experimental IR spectrum the latter can be assigned, as detailed in Figures 4 and 5 and Table 1 of Supporting Information. Note that, as expected,²² calculated frequencies are a few percent greater than experimental frequencies due to the neglect of anharmonicity in the calculations. Experimental bands are assigned to (1) fundamentals of **1**; or (2) overtone/combination bands of **1**; or (3) impurities. As is seen in Figure 4, the vast majority of observed bands in the experimental spectrum can be assigned to fundamentals of **1**. We note that conformational splittings are clearly observable for modes 13, 20, 28, and 45. The observed splittings, 27, 7, 8, and 5 cm⁻¹, are in good agreement with the calculated splittings, 25, 2, 8, and 6 cm⁻¹, for these modes. The relative intensities of the bands of *E*- and *Z*-**1** for these modes are qualitatively consistent with prediction.

Given the assignment of the IR spectrum of **1**, we can accomplish the goal of this work, namely to determine

the AC of **1** via comparison of the predicted VCD and the experimental VCD. Mid-IR VCD spectra of *E*- and *Z*-**1** predicted using B3PW91 and TZ2P are shown in Figure 6 for *S*-**1**. VCD intensities are determined by vibrational rotational strengths. The calculated rotational strengths are given in Table 1 of Supporting Information. Lorentzian band shapes are again used in synthesizing VCD spectra. The spectrum of the conformational mixture is shown in Figures 5 and 6. B3PW91/TZ2P rotational strengths of *E*- and *Z*-**1** differ much more than do the dipole strengths. As a result, the B3PW91/TZ2P VCD spectra of *E*- and *Z*-**1** differ much more than do the absorption spectra. Due to the greater population of the *Z* conformation, the *E/Z* spectrum is qualitatively similar to the *Z* spectrum. However, for modes 33, 34, 38, 43, 47–50, and 54, differences are clearly visible due to the presence of the *E* conformation. As seen in Figures 5 and 6, the B3PW91/TZ2P *E/Z* VCD spectrum of *S*-**1** is in excellent agreement overall with the experimental spectrum of (–)-**1**. For modes 29–39, 41, 45–47, and 51–53, VCD is clearly observable. All signs are correctly predicted and relative intensities are in qualitative agreement with theory. Note, in particular, that the predicted anisotropy ratios of modes 31 and 39 are 2.1×10^{-4} and -0.9×10^{-4} , respectively, in excellent agreement with the experimental values of 2.7×10^{-4} and -0.9×10^{-4} . The excellent agreement of the calculated VCD for *S*-**1** with the experimental VCD for (–)-**1** unambiguously defines the absolute configuration of **1** as *R*(+)/*S*(–).

(+)-**1** and (–)-**1** resulted from sulfoxidation catalyzed by (*S,S*)-DPED and (*R,R*)-DPED, respectively. Given the *R*(+)/*S*(–) AC of **1**, established above, it follows that (*R,R*)- and (*S,S*)-DPED yield *S*-**1** and *R*-**1** respectively. Prior syntheses of alkyl aryl sulfoxides using Ti(*i*-PrO)₄/H₂O/DPED mediated catalytic sulfoxidation with (*R,R*)-DPED have uniformly yielded sulfoxides of *S*AC.^{13f,18} The results reported here provide further support for the

(22) Finley, J. W.; Stephens, P. J. *J. Mol. Struct. (THEOCHEM)* **1995**, *357*, 225.

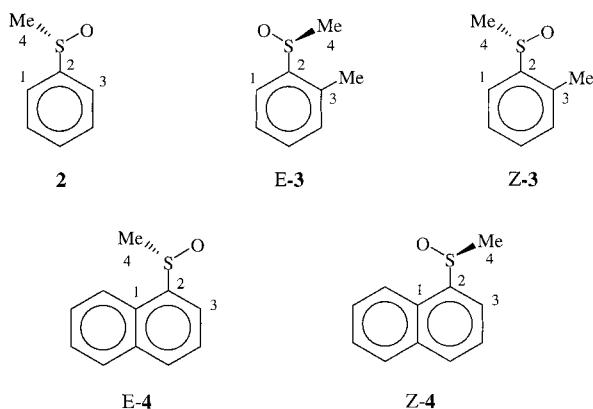
Table 3. B3PW91/TZ2P Dihedral Angles for 1–4^a

coordinates ^b	OSC2C1 ^b	OSC2C3 ^b	C4SC2C1 ^b	C4SC2C3 ^b
<i>E</i> -1	144.7	-32.8	-103.9	78.6
<i>Z</i> -1	-34.4	145.5	76.6	-103.6
2	171.2	-5.3	-79.6	103.9
<i>E</i> -3	-8.0	167.7	100.9	-83.4
<i>Z</i> -3	142.1	-34.8	-106.7	76.3
<i>E</i> -4	169.9	-6.9	-81.4	101.8
<i>Z</i> -4	-35.1	145.1	75.5	-104.3

^a Dihedral angles are in degrees and for *S* absolute configurations. ^b Atom numbering is indicated in the text.

general conclusion that, for this catalytic protocol, the AC of the sulfoxide product depends only on the AC of the chiral inducer. This correlation will be of practical value in further applications of this methodology.

Prediction of the structures and the energy difference of the conformations of **1** is prerequisite for the prediction of its IR and VCD spectra. The excellent agreement of the B3PW91/TZ2P *E/Z* IR and VCD spectra with the experimental spectra (given the correct choice of AC in the case of the VCD spectrum) demonstrates the reliability of the B3PW91/TZ2P structures and energies of the *E* and *Z* conformations. We now consider these properties of **1** in more detail, by comparison with the structurally related sulfoxides **2**–**4**.



In both *E*- and *Z*-**1** the S–O group is rotated by 30–40° from coplanarity with the naphthyl moiety. In phenylmethyl sulfoxide, **2**, B3PW91/TZ2P calculations predict that the S–O group is nearly coplanar with the phenyl ring; the deviation from coplanarity is <10° (see Table 3). It is clear that in *E*- and *Z*-**1** the much greater deviation from coplanarity of the S–O and naphthyl groups is caused by steric repulsion between the sulfoxide O atom and, in *E*-**1**, the methyl substituent on the naphthyl group and, in *Z*-**1**, the peri-H of the naphthyl group. This conclusion is supported by B3PW91/TZ2P calculations on *o*-tolyl methyl sulfoxide, **3**, and 1-naphthyl methyl sulfoxide, **4**. Structural parameters for **3** and **4** are given in Table 3. In *E*-**3** the orientation of the S–O group is very similar to that in **2**. In *Z*-**3**, the S–O group is rotated away from coplanarity due to steric hindrance by the *o*-methyl substituent. The deviation from coplanarity is very similar to that in *E*-**1**. In *E*-**4**, the orientation of the S–O group is very similar to that in **2**. In *Z*-**4**, the S–O group is rotated away from coplanarity due to steric hindrance with the peri-H atom of the naphthyl group. The deviation from coplanarity is very similar to that in *Z*-**1**.

This analysis can be extended to the energy difference of *E*- and *Z*-**1**. In **3**, the B3PW91/TZ2P energy difference

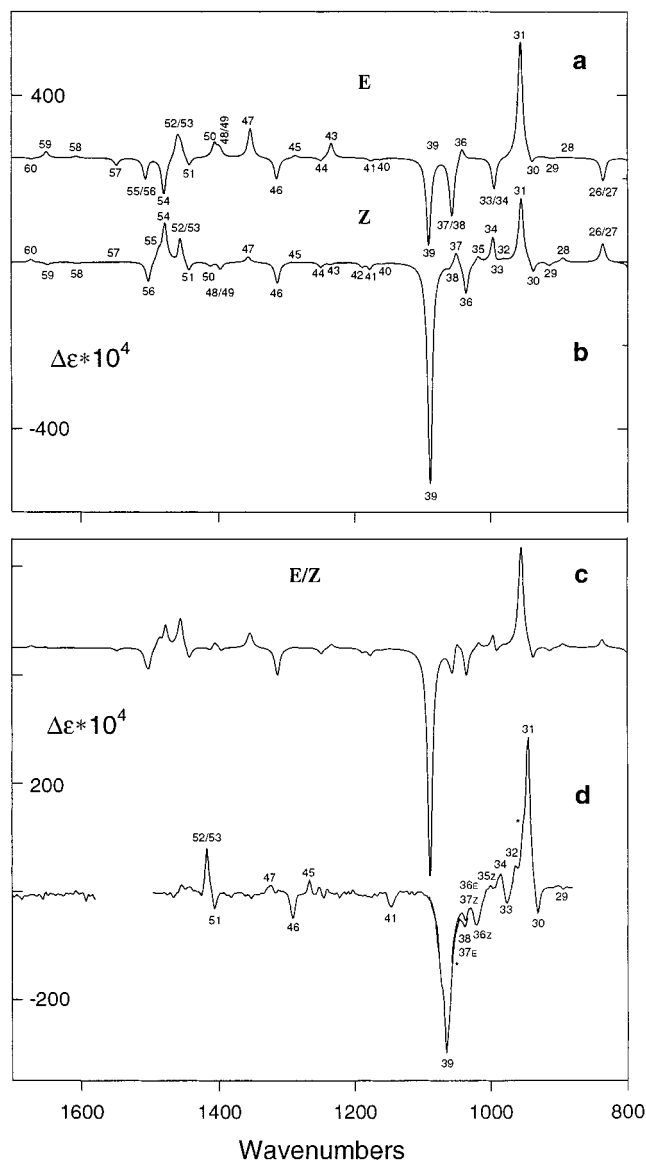


Figure 6. Mid-IR VCD spectra of **1**. **a**: B3PW91/TZ2P spectrum of *E*-**1**; **b**: B3PW91/TZ2P spectrum of *Z*-**1**; **c**: B3PW91/TZ2P *E/Z* spectrum; **d**: experimental spectrum (from Figure 1). In **a** and **b** band shapes are Lorentzian; $\gamma = 4.0 \text{ cm}^{-1}$. The spectrum in **c** is obtained from those in **a** and **b** using populations of *E*- and *Z*-**1** calculated from their B3PW91/TZ2P energies (Table 2). Fundamentals are numbered. In **d**, where *E* and *Z* bands are not resolved, the numbering refers to both *E* and *Z* conformations. In **d**, asterisks indicate bands not assignable to fundamentals of **1** and attributable to either overtone/combination bands of **1** or impurities. Calculated spectra are for *S*-**1**; the experimental spectrum is for (–)-**1**.

of *E* and *Z* conformations is ~2.2 kcal/mol, *E* being lower in energy (Table 2). In **4**, the B3PW91/TZ2P energy difference of *E* and *Z* conformations is ~1.8 kcal/mol, *E* being lower in energy (Table 2). Assuming that the steric repulsion energies in *E*- and *Z*-**1** are the same as *Z*-**3** and *Z*-**4** respectively, it follows that *Z*-**1** should be lower in energy than *E*-**1** by ~0.4 kcal/mol, a value in excellent agreement with the directly calculated B3PW91/TZ2P value of ~0.5 kcal/mol.

Conclusion

Our study of **1** provides a practical demonstration of the application of VCD spectroscopy to the determination

of the AC of a chiral molecule. Methods for the determination of AC already exist. However, VCD spectroscopy offers a number of advantages. First, it is a *direct* method, applicable without reference to other chiral molecules. Second, it is a *solution* method, not requiring single crystals. Third, it is *rapid*. Experimental spectra can be measured in hours. Spectra can be calculated (for medium-sized molecules) in hours (given state-of-the-art computational hardware) simultaneously. Last, it is straightforwardly implemented by the nonspecialist. A commercial FT VCD spectrometer is no more difficult to use than a commercial FT IR spectrometer. Computations are carried out using a standard ab initio quantum chemistry package. For many molecules, VCD spectroscopy should thus provide an attractive alternative to other methods for determining AC.

Experimental Methods

Synthesis. Enantiomeric excess was determined by HPLC analysis at room temperature on Daicel Chiralcel OD chiral stationary phase ($\lambda = 254$ nm, flow 1.0 mL/min, eluent 95:5 hexane: i -PrOH). ^1H NMR (300 MHz) and ^{13}C NMR spectra were recorded in CDCl_3 . Optical rotations were measured with a JASCO DIP-370 digital polarimeter. CCl_4 was distilled from CaH_2 and stored over activated 4 Å molecular sieves. $\text{Ti}(i\text{-PrO})_4$ (Aldrich) was distilled prior to use under a N_2 atmosphere. Commercially available *tert*-butyl hydroperoxide (TBHP) (70% in water) was purchased (Aldrich) and used without further purification. Analytical TLC was performed on 0.2 mm Merck 60 F-254 silica gel plates and column chromatography was carried out with Merck 60 (80–230 mesh) silica gel. Enantiomerically pure (*R,R*)- and (*S,S*)-1,2-diphenylethane-1,2-diol (DPED) were prepared by asymmetric dihydroxylation of (*E*)-stilbene.²³ 1-(2-Methylnaphthyl) methyl sulfide was prepared according to a literature procedure,²⁴ starting from 1-bromo-2-methylnaphthalene. Racemic sulfoxide, (\pm)-**1**, was prepared by oxidation of this sulfide with 30% hydrogen peroxide, according to a literature procedure.²⁵

1-(2-Methylnaphthyl) methyl sulfide: ^1H NMR (CDCl_3 , 300 MHz) δ 2.31 (s, 3H), 2.78 (s, 3H), 7.40 (d, $J = 8.3$ Hz, 1H), 7.46 (m, 1H), 7.59 (m, 1H), 7.74 (d, $J = 8.3$ Hz, 1H), 7.82 (d, $J = 8.3$ Hz, 1H), 8.70 (d, $J = 8.3$ Hz, 1H); ^{13}C NMR (CDCl_3 , 75 MHz) δ 19.00, 22.04, 125.08, 126.17, 126.79, 128.37, 128.70, 131.90, 132.83, 135.01, 141.03.

(-)-1-(2-Methylnaphthyl) Methyl Sulfoxide (1). To a suspension of (*R,R*)-DPED (34.3 mg, 0.16 mmol) in CCl_4 (5 mL) were dropwise added in sequence $\text{Ti}(i\text{-PrO})_4$ (23.6 μL , 0.08 mmol) and H_2O (28.8 μL , 1.6 mmol). To the resulting homogeneous solution was added 1-(2-methylnaphthyl) methyl sulfide (1.61 mmol), stirring at room temperature for 15 min. The solution was then cooled at 0 °C, and TBHP (70% in water, 440 μL , 3.22 mmol) added. The mixture was left stirring at 0 °C for 2 h and then diluted with CH_2Cl_2 and dried over Na_2CO_3 .

(23) Kolb, H. C.; Van Nieuwenhze, M. S.; Sharpless, K. B. *Chem. Rev.* **1994**, *94*, 2483.

(24) Czarnik, A. W. *J. Org. Chem.* **1984**, *49*, 924.

(25) Lupattelli, P.; Ruzziconi, R.; Scafato, P.; Degl'Innocenti A.; Belli Paolobelli, A. *Synth. Commun.* **1997**, *27*, 441.

SO_4 for a few minutes. After filtration and evaporation of the solvent, the residue was immediately purified by column chromatography (EtOAc), isolating 148 mg of pure **1** in 45% yield as a viscous liquid: $t_r(\text{S}) = 33.0$ min, $t_r(\text{R}) = 38.7$ min; ee = 60%; $[\alpha]_D^{20} = -66.2^\circ$ ($c = 0.54$, acetone); ^1H NMR (CDCl_3 , 300 MHz) δ 2.73 (s, 3H), 3.04 (s, 3H), 7.48 (d, $J = 7.6$ Hz, 1H), 7.5–7.7 (m, 2H), 7.83 (d, $J = 8.4$ Hz, 1H), 7.86 (d, $J = 7.9$ Hz, 1H), 9.08 (d, $J = 8.4$ Hz, 1H); ^{13}C NMR (CDCl_3 , 75 MHz) δ 19.24, 38.77, 122.90, 125.72, 127.03, 128.79, 129.07, 130.40, 131.58, 132.97, 134.95, 136.29.

(+)-1-(2-Methylnaphthyl) Methyl Sulfoxide (1). The above procedure was used employing (*S,S*)-DPED as the chiral ligand, affording (+)-**1** in 50% yield and ee = 50%.

Spectroscopy. Vibrational unpolarized absorption ("IR") spectra of (+)-, (-)-, and (\pm)-**1** were measured in CCl_4 solution using a Nicolet MX-1 spectrometer at 1 cm^{-1} resolution. The IR spectra of (+)-, (-)-, and (\pm)-**1** were very similar, indicating comparable chemical purities. Variations indicated that the (\pm)-**1** sample was slightly more pure than the (+)- and (-)-**1** samples. VCD spectra of (+)- and (-)-**1** were measured in CCl_4 solution using a Bomem/BioTools Chiral IR spectrometer at 4 cm^{-1} resolution. Scan times were 1 h. Baselines were provided by (\pm)-**1** solutions. After conversion to $\Delta\epsilon$ units, VCD spectra of (+)- and (-)-**1** were normalized to 100% ee and the "half-difference" spectrum calculated: $1/2[\Delta\epsilon(-) - \Delta\epsilon(+)]$, to obtain the final VCD spectrum of (-)-**1**. IR and VCD spectra were measured at concentrations of **1** of ~ 0.1 M. IR spectra at ~ 0.01 M and ~ 0.1 M concentrations are superposable, demonstrating the absence of dimerization/aggregation at ~ 0.1 M concentrations.

Calculations. Ab initio DFT calculations were carried out using GAUSSIAN 98.⁸ The hybrid functional, B3PW91¹⁹ and two basis sets, 6-31G*²⁰ and TZ2P,²¹ were used. The B3PW91 functional has been shown to provide vibrational spectra for phenyl methyl and naphthyl methyl sulfoxides superior to those obtained using B3LYP^{15b} and is accordingly the functional selected in the case of **1**. Harmonic force fields (HFFs), atomic polar tensors (APT), and atomic axial tensors (AATs) were calculated using direct analytical derivative (AD) methods and perturbation-dependent (PD) basis sets.^{1,4,26} In the case of AATs, gauge-invariant atomic orbitals (GIAOs) were used.⁴ Harmonic vibrational frequencies, dipole strengths, and rotational strengths were calculated thence. IR and VCD spectra were calculated using Lorentzian band shapes.^{5b,c}

Acknowledgment. Financial support by NSF (CHE-9902832) to P. J. S., Elf Aquitaine/Sanofi to A.A., and by Università della Basilicata (Potenza) and MURST (Rome) to C.R., S.S., and M.I.D. is gratefully acknowledged.

Supporting Information Available: Calculated and experimental vibrational frequencies, dipole strengths, and rotational strengths are given in Table 1. This material is free of charge via the Internet at <http://pubs.acs.org>.

JO001403K

(26) Stephens, P. J. *Encyclopedia of Spectroscopy and Spectrometry*; Academic Press: London, 1999; p 2415.